Optics Communications 349 (2015) 203–208

Contents lists available at ScienceDirect

Optics Communications

journal homepage: www.elsevier.com/locate/optcom

Polarization of vector solitons generated in break-up process in twisted fiber

Y. E. Bracamontes-Rodríguez [a,*], I. Armas Rivera [a], G. Beltrán-Pérez [a], O. Pottiez [b], B. Ibarra-Escamilla [c], M. Durán-Sánchez [c,d], E. A. Kuzin [c]

[a] BUAP, Facultad de Ciencias Físico Matemáticas, Av. San Claudio y 18 Sur, San Manuel, Puebla, México
[b] Centro de Investigaciones en Óptica, Loma del Bosque 115, Col. Lomas del Campestre, León, Gto 37150, México
[c] INAOE, Enrique Erro 1, Tonantzintla A.P., 72000, Puebla, México
[d] Consejo Nacional de Ciencia y Tecnología (CONACYT), Av. Insurgentes Sur No. 1582, Col. Crédito Constructor, Del. Benito Juárez, C. P. 039040, México D. F.

ARTICLE INFO

Article history:
Received 17 December 2014
Received in revised form
13 March 2015
Accepted 14 March 2015
Available online 27 March 2015

Keywords:
Nonlinear optics
Fiber
Pulse propagation and temporal solitons

ABSTRACT

We study experimentally the polarization of the radiation resulting from the pulse break-up process in a SMF-28 twisted fiber. The fiber twist causes circular birefringence and also mitigates the linear birefringence. The twisted fiber may be considered for nonlinear effect as fiber without linear birefringence, which allows the investigation of polarization properties which cannot be studied in common fibers because of the random residual birefringence. We found that the polarization of the formed solitons is more stable when the input pump polarization has elliptical polarization with big angle of ellipticity. At input polarization close to linear we observed that the polarization ellipticity angle tends to be higher than the polarization ellipticity angle of the input pump. The fluctuation of the polarization grows when the input polarization approaches to the linear.

1. Introduction

Solitons as the exact solution of the Nonlinear Schrödinger Equation (NLSE) can be found for linearly or circularly polarized light [1] in fibers without birefringence. In practice the polarization is not conserved along the fiber because of fiber birefringence. However, even in the fiber with birefringence the pulse can propagate stably in the form of the vector soliton. The concept of vector soliton has been intensively discussed. It was shown that the nonlinear coupling between orthogonally polarized modes allows their envelopes to propagate without temporal walk-off forming the so-called group-velocity locked vector soliton [2, 3]. Also the phase locked vector soliton was found [4, 5]. The concept of the vector solitons was considered for fiber lasers [6–8]. In the papers cited above a single vector soliton propagating in the fiber was discussed.

A pulse with power much higher than the soliton in a fiber with anomalous dispersion becomes instable and transforms into a number of solitons. The initial dynamic of this process depends on pulse duration and for long pulses (ps and longer) modulation instability plays an important role. In the time domain, these processes induce a fast modulation of the pump envelope which can subsequently break up into a train of femtosecond solitons. The fact that the initial dynamics is seeded from noise results in random fluctuation of the solitons parameters. The pulse break-up is one of the principal mechanisms of formation of supercontinuum [9] and also may play important role in the formation of noise-like pulses in fiber lasers [10–12]. The mechanism of the formation of noise like pulses is not yet well established.

The polarization properties of vector solitons generated in the break-up process have been investigated in relation with SC generation because the polarization stability can be an important issue for applications [13–17]. Numerical simulations for the fiber with low birefringence [13] show that the output polarization depends randomly on the wavelength even without imposed noise if the input polarization is aligned at an angle of 45° to the slow axis. When the input was linearly polarized close to the slow axis the SC output had the slow axis polarization dominant, with few components present in the fast mode. However, for input polarized close to the fast axis the output polarization was random. The noise imposed on the pulse results in random polarization at the fiber output. The fluctuations depend on pulse duration and become lower when the pulse is shorter. The calculations were done for pulses with durations of 150 fs and shorter.

A commonly accepted way to stabilize the polarization of SC is the use of fibers with high birefringence [15, 17].However the application of hi-bi fibers may be limited. One example is provided by mode-locked fiber lasers where the principal mechanism of mode-locking is nonlinear polarization rotation [18, 19]. Another

* Corresponding author.

http://dx.doi.org/10.1016/j.optcom.2015.03.030
0030-4018/

way to provide polarization stability is introducing circular birefringence by fiber twist. In combination with the linear birefringence, elliptical birefringence results and causes a rather complicated evolution of the polarization [20, 21]. However, if the circular birefringence is much higher than the linear birefringence, the linear birefringence is mitigated and the fiber has circular birefringence. Moreover for nonlinear processes the twisted fiber may be considered as a perfectly isotropic fiber [22] useful for the investigation of nonlinear processes. The investigation of soliton formation and soliton propagation in a twisted fiber may reveal effects that are normally disguised by the presence of residual linear birefringence.

However, there are only a few papers where the formation and evolution of vector solitons in a twisted fiber were investigated. One of the new effects discovered recently was reported in [23]. It was shown theoretically that the polarization of Raman solitons evolves towards circular during the propagation in a fiber with circular birefringence if the vectorial nature of the Raman effect is taken into account. The comparison of the polarization of the radiation formed in a twisted fiber and in a fiber without intentionally introduced twist was discussed previously in [22]. In fibers without twist and hence with residual linear birefringence the polarization was completely random at any input polarization. In contrast, the polarization of the radiation in twisted fibers shows some stability especially if input polarization is circular. It was also suggested that if the input polarization is close to linear the output polarization tends to have an ellipticity angle greater that the ellipticity angle of the input pulse. In this paper ns pulses were used for pumping. In that case the number of pulses formed by pulse break-up is very large and the time separation between pulses with different wavelengths is less than the pump pulse duration. So the process of the formation of separate solitons was not terminated.

In the present paper we used 0.7-ps pulses generated by a fiber ring laser. The calculations show that for sub-ps pulses the longer-wavelength part of the spectrum at the fiber output consists of solitons separated in space. We measured the polarization of solitons at the end of a 500-m twisted SMF-28 fiber using a single shot technique. This technique also allows measuring the fluctuations of the polarization. To the best of our knowledge it was never done before. We find that solitons have a more stable polarization if the input pulses have polarization close to circular. At input pulse polarization close to linear the fluctuation grows significantly and the output ellipticity tends to be greater than the input ellipticity.

2. Experimental setup

The experimental setup is presented in Fig. 1a. As a source of signal we used a mode-locked fiber ring laser based on nonlinear polarization rotation, Fig. 1b. The laser cavity consists of a 3-m EDF with normal dispersion and 10 m of the standard fiber Corning SMF-28. The cavity also includes a WDM, the output coupler and free space elements: a half wave plate (HWP), a polarization-dependent isolator and a quarter wave plate (QWP). The configuration is typical for soliton lasers. The length of the cavity is 14 m with a total anomalous dispersion estimated as -0.25 ps^2. The rotation of the HWP and QWP changes the generation regime. We used pulses with spectra shown in the Fig. 2a and Fig. 2b. In the first case the spectrum bandwidth was 5.5 nm with 1544 nm central wavelength and the autocorrelation function of 1.3 ps. The spectrum assumes that the pulse may have some internal structure or chirp. The spectrum shown in the Fig. 2a is typical for soliton lasers. The central wavelength is 1532 nm; bandwidth is 7.3 nm. The FWHM of the autocorrelation function is 0.4 ps.

The pulses from the laser were stretched by the 12-m SMF-28 fiber and then amplified by an EDFA with maximum amplification of 150 times. The pulses from the amplifier output pass through a polarization controller (PC), a polarizer, and a quarter wave retarder (QWR1). Rotation of the QWR1 allows stable polarization with desirable ellipticity at the input of the twisted SMF-28 fiber. It has to be note that the spectra generated in the twisted fiber were different for two regime of the laser. The pulse with spectrum shown in the Fig. 2a generated the broadband flat spectrum consisting of multiple solitons, while the pulse with the spectrum shown in the Fig. 2b generated one or few number of well separated solitons. The details will be discussed below. We used two spans of the fibers with lengths of 500 m and 200 m. The fiber in both spans were twisted with a twist rate of 7 turns/meter and placed on a cylinder with a diameter of 46 cm. The dispersion of the fiber is 25 ps^2/km and nonlinearity is approximated by 1.5 (W-km)$^{-1}$. For our purpose the linear birefringence has to be mitigated by the fiber twist. To do this the circular birefringence has to be much larger than the linear. It was shown [20] that the twist introduces an optical activity proportional to the twist:

$$\alpha = g\tau L, \tag{1}$$

where τ is the fiber twist rate. The coefficient g was calculated from the elastooptic tensor for silica glass to be approximately of 0.16. This value depends slightly on the doping concentration. However even for highly doped fiber it gives a good correspondence with experimental results [21]. The difference between refractive indexes for orthogonal circularly polarized beams is defined by:

$$\Delta n_c = \frac{\lambda}{2\pi} g\tau, \tag{2}$$

where Δn_c is the difference between refractive indexes for orthogonal circularly polarized waves. This equation yields the value of Δn_c equal to 1.7×10^{-6} for a wavelength of 1.55 μm and a twist rate of 7 turns/m. The beat length for the same fiber without bending was measured as 15 m [25] that corresponds to a value of Δn_l for orthogonal linearly polarized beams equal to 10^{-7}. Fiber twist also causes polarization mode dispersion. It can be calculated from:

$$\Delta t_c = \frac{L}{c}\tau\frac{dg}{dk}, \tag{3}$$

where k is the wave number. Using the dependence of the coefficient "g" on the wavelength [26] we obtain that for the twist rate of 7 turns/m the polarization mode dispersion is equal to 0.3 ps/km.

Linear birefringence in single-mode optical fibers results also from fiber bend [27]. For the bend diameter of 46 cm Δn_l is equal to 3.4×10^{-8}. We can see that for our coil the circular birefringence resulting from twist is at least one order of magnitude higher than linear birefringence. However, there may be some additional effects such as additional stress in the process of coiling which can causes the linear birefringence. However it is impossible to cancel completely the linear birefringence and ellipticity of the pulse is change slightly in the fiber. It is not very important for circular input polarization because the polarization along all fiber length remains close to circular, however in may be very important for linear input polarization because even small ellipticity changes can change the sigh of the ellipticity angle.

The fiber output is connected to a circular polarizer formed by QWR2 and a polarizer. The QWR2 converts orthogonally polarized circular components at the fiber output into orthogonally polarized linear components. The linearly polarized components are then splitted by a fiber polarization beam splitter (PBS). The pulses

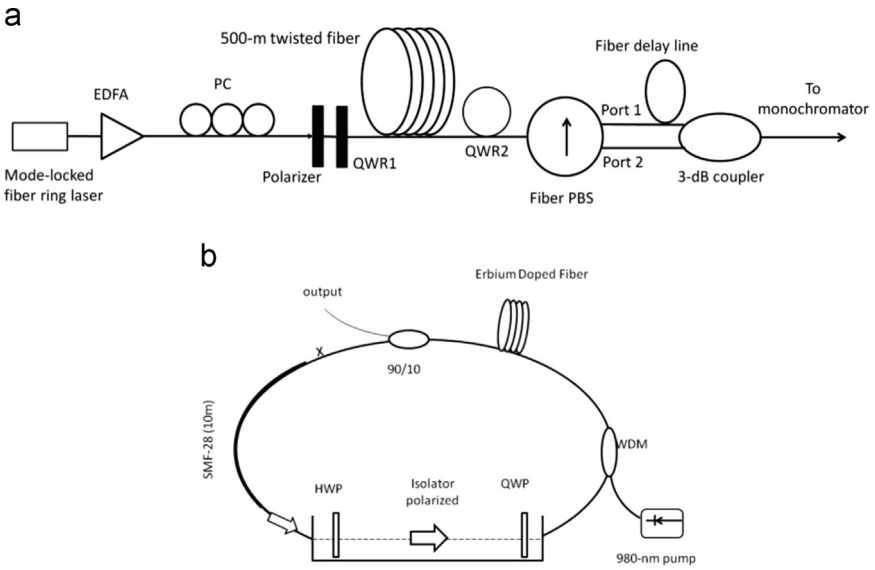

Fig. 1. Experimental setup (a), the mode-locked fiber laser used in the experiment (b).

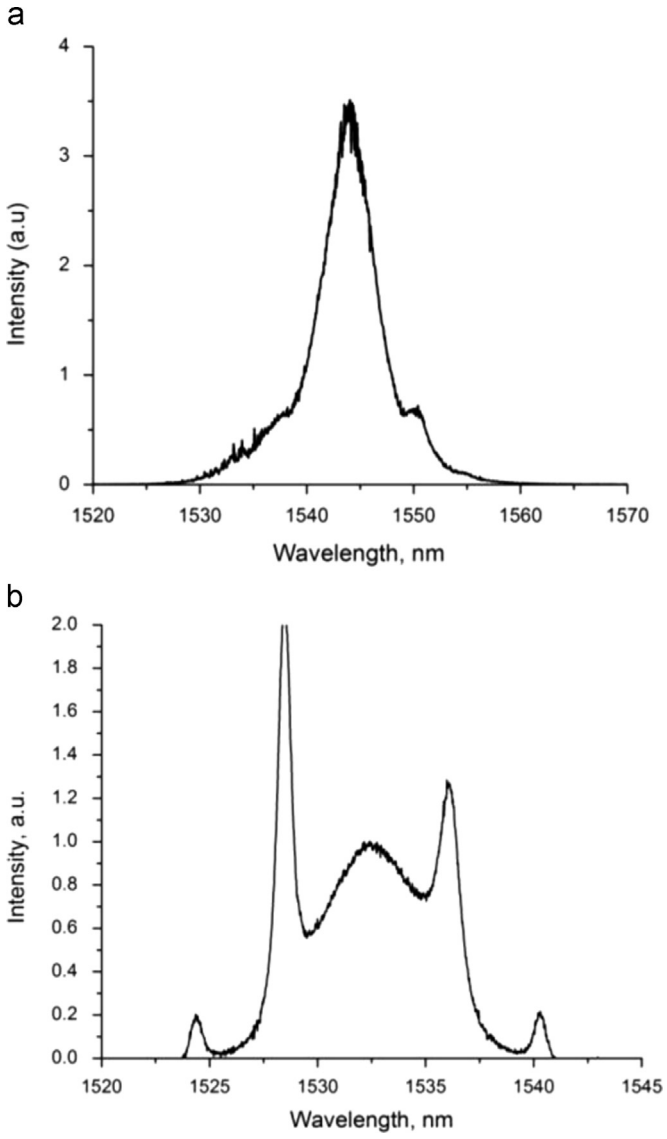

Fig. 2. Spectra of the laser pulses used in the experiment.

at the PBS outputs are shifted in time by a delay line and then using a 50/50 coupler they are combined and launched to a monochromator. The delay between pulses was 65 ns, this value was chosen in order to have the possibility to observe both pulses without interference between them in single shot regime. The pulses are then detected by a photodetector with a bandwidth of 800 MHz and monitored by an oscilloscope. The amplitudes of the detected pulses are proportional to the orthogonally polarized circular components at the fiber output. With this setup we are able to measure the amplitudes of the left- and right-circularly polarized components at a selected wavelength in one single shot. The ellipticity is then calculated using the equation:

$$\rho = \tan^{-1}\left(\frac{\sqrt{P_+} - \sqrt{P_-}}{\sqrt{P_+} + \sqrt{P_-}}\right), \tag{4}$$

where P_+ and P_- are the pulse amplitudes at the monochromator output. The details of the procedure of the ellipticity measurement can be found in [24].

3. Results and discussions

Firstly we used the 500-m fiber and the pulses with spectrum

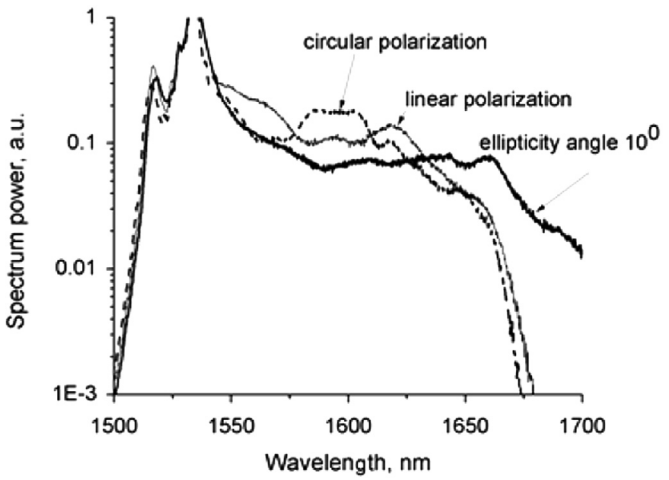

Fig. 3. Spectra at the 500-m fiber output at different input polarizations.

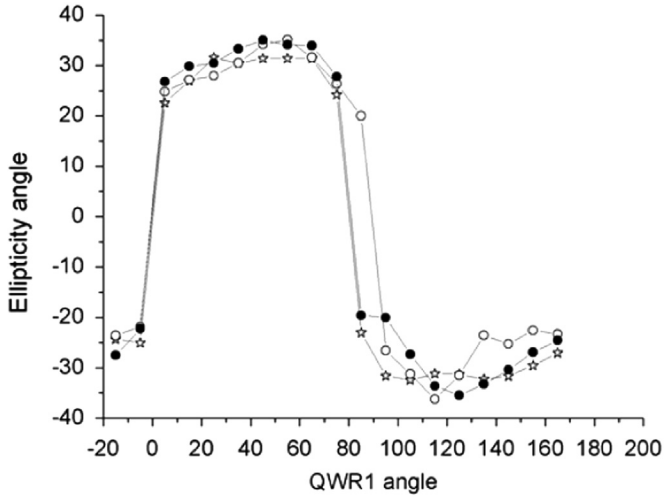

Fig. 4. Ellipticity angle of the output for 1545 nm, open circles, 1550 nm closed circles, and 1630 nm, stars.

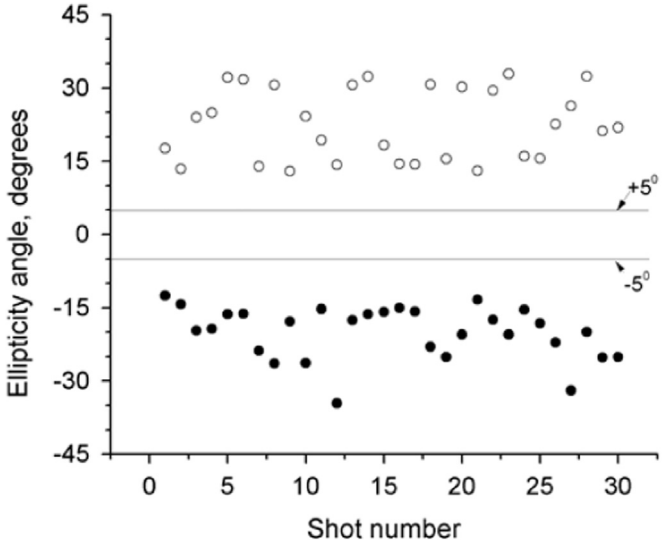

Fig. 5. Results of the single shot measurements at polarization angles of input pulse $+5°$ (open circles) and $-5°$ (closed circles).

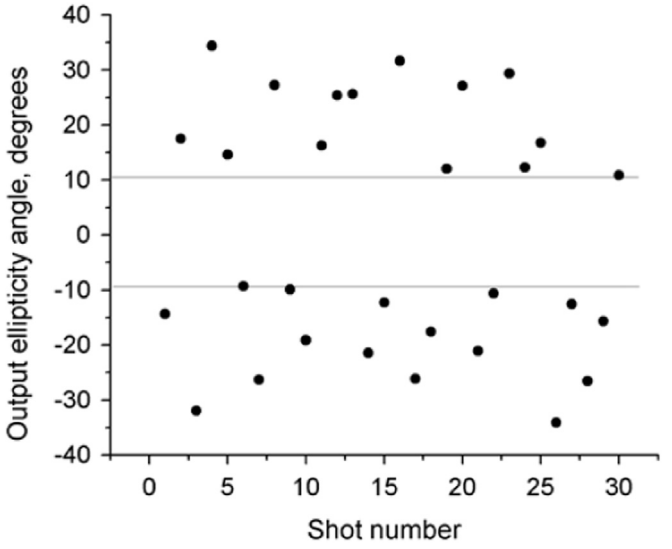

Fig. 6. Results of the single shot measurements at linear input polarization (QWR angle 90°).

shown in the Fig. 2a. The spectra at the fiber output at different ellipticity angles are shown in Fig. 3. We can see some difference between the spectra depending on the input polarization. We measured the output ellipticity at 1630 nm, 1550 nm, and 1545 nm. The wavelength 1630 nm lies in the range of the longest wavelengths where intense signal exists at any input polarization; 1550 nm is slightly higher than the central pump wavelength, and 1545 nm coincides with the central wavelength. The dependences of output ellipticity angle on the QWR1 angle are shown in Fig. 4. For the QWR1 angle between 0° and 45° the ellipticity angle of the pump pulse is equal to the QWR1 angle, and for QWR1 angle between 45° and 90° the ellipticity angle is equal to 90° minus the QWR1 angle. For all wavelengths we observe a similar dependence with a flat top and a steep jump at the input polarization close to linear (QWR1 angles 0° and 90°). The flat top was observed over a wide range of the input ellipticity angle from 5° to 45°. At circular polarization of the input pulse (QWR1 angles of 45° and 135°) the ellipticity approaches 35° or -35°, which is close to circular polarization. Similar results were obtained for ns pump pulses [24]. It was mentioned in that reference that the ellipticity angle at the fiber output seems to be larger than the ellipticity angle of the pump at polarization close to linear. For ps-duration pump this effect can be seen very clearly.

Very interesting is the jump between positive and negative ellipticities for input polarization close to linear. In order to appreciate the details we made 30 single shot measurements at the wavelength of 1630 nm for each ellipticity of the pump and calculated the output ellipticity angle. Fig. 5 shows the results for input pulses with an ellipticity angle of $+5°$ (open circles) and $-5°$ (closed circles). QWR1 angles are equal to 85° and 95° respectively for these results. Solid lines show the reference of $+5°$ and $-5°$. We see that for all measurements the solitons at the fiber output have a polarization more elliptical than the pump pulse. For a pump pulse ellipticity angle of 5° the average ellipticity at the output is 22°; for $-5°$ the average ellipticity is $-20°$.

At linear input pulse polarization we have found that all the results can be separated into two groups, one with a positive ellipticity angle higher than 10° and another with a negative ellipticity angle whose module is also higher than 10°, see Fig. 6. Between these groups we can clearly see the gap. The average ellipticity for positive ellipticity angles is 15.9°; the average ellipticity for negative ellipticity angles is $-16.8°$. None of the measurements shows an ellipticity angle between $+10°$ and $-10°$. However the average between all measurements will give an average ellipticity of -0.45, which is very close to linear polarization. A similar distribution of soliton ellipticities was probably prevailing in the previously published paper using ns pulses as the pump, where the ellipticity was averaged between a very large number of solitons [23].

The single shot results for different ellipticity angles of the pump pulse are summarized in Fig. 7. All points in this figure except those at linear input polarization (QWR angle 90° and 180°) are obtained by averaging 30 single shot measurements. For linear input polarization we averaged separately the results with positive and negative ellipticity angles.

The single shot results allow the calculation of the standard deviation of the soliton ellipticity angles for different input ellipticity angles. The result is shown in Fig. 8. Here we can see that the standard deviation has a minimum when the input polarization is circular (QWR1 angle is equal to 135°) and presents strong maxima when the input polarization is linear.

The results of our measurements show that the polarization of solitons generated in the process of soliton fission is unstable even in a fiber without residual linear birefringence. The instability

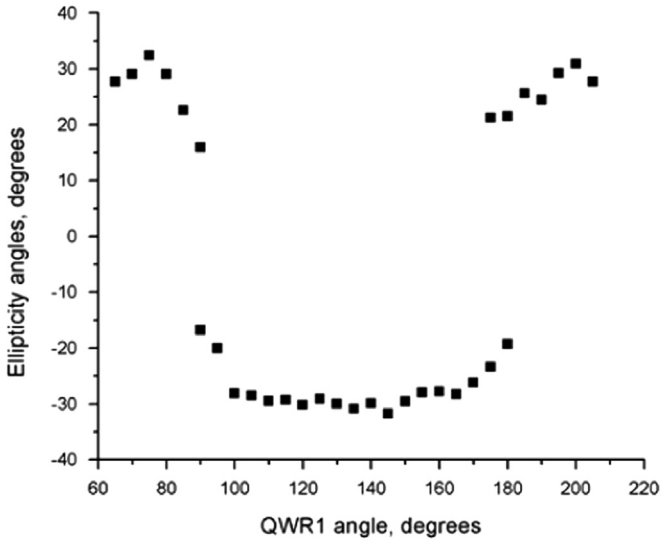

Fig. 7. Ellipticity of the solitons centered at 1630 nm.

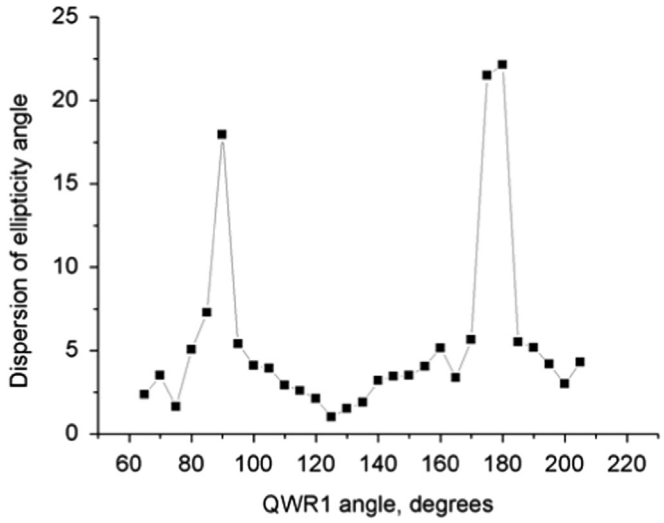

Fig. 8. Dispersion of the ellipticity angle.

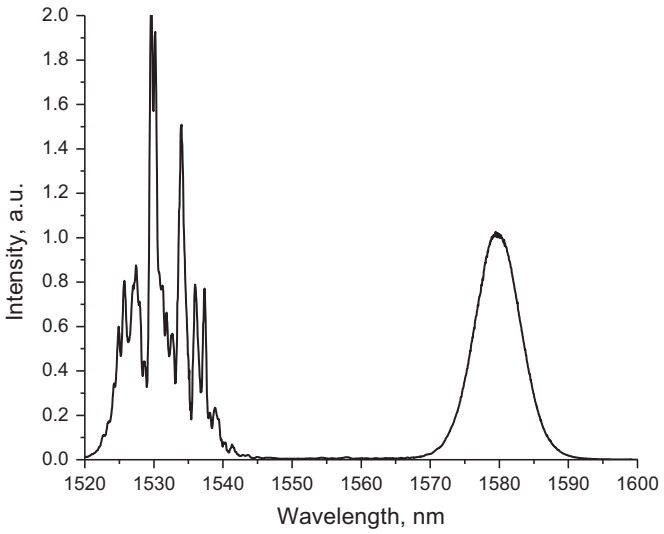

Fig.9. Typical spectrum at the fiber output.

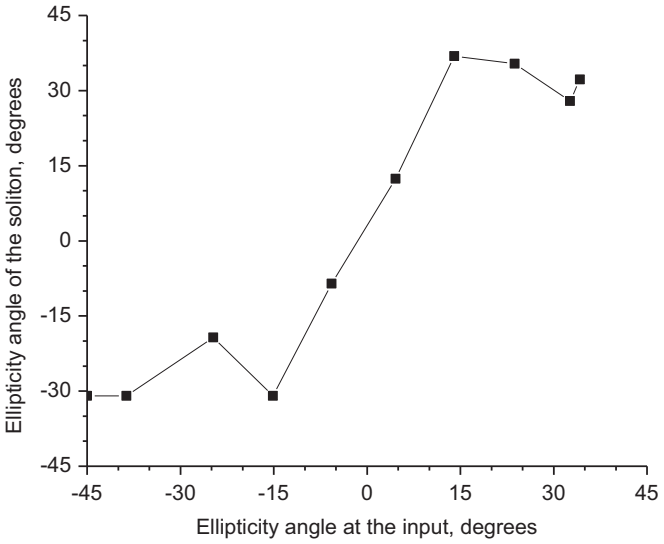

Fig. 10. The dependence of the output ellipticity on the input for the 200-m fiber.

grows strongly when the input pulse has linear polarization. The minimum instability was observed at circular polarization of the input pulse. It has to be noted that very similar results were obtained for left- and right- elliptically polarized input pulses. The fact that the polarization does not reach exactly the circular polarization even with circular polarization of the input pulse may be attributed to the fact that the process of broad band spectrum generation involves a complex set of nonlinear processes, not only soliton formation. However our experimental technique does not allow the separation of solitons from other components.

When the fiber ring laser was adjusted to have the spectrum shown in Fig. 2b we were able to generate in twisted fiber a single soliton moving to longer wavelengths by Raman SFS. We used the 200-m fiber for this set of measurements. The typical spectrum at the fiber output is shown in the Fig. 9. The single soliton is centered at 1577 nm and has the bandwidth of 11.9 nm. This bandwidth yields the soliton duration of 0.21 ps. The central wavelength strongly depended on the pump power.

The dependence of the output polarization ellipticity on the input is shown in the Fig. 10. We see fast change of the output ellipticity angle from approximately left-hand circular to right-hand circular when input polarization angle is change from -15° to 15°. The measurements at polarization close to linear can be complicated by even very small amount of linear birefringence because of possible change of the ellipticity angle sign. We implemented the measurements with linear input polarization. In this set of the experiments we removed the QWR1 and rotated the polarizer. The measurements at low power showed that the polarization at the fiber output oscillates between $+10^\circ$ and -10° depending on the input polarization angle. This gives the possible range of the ellipticity oscillation along the fiber. The polarization dependence on the input angle for the single soliton at the fiber output is shown in the Fig. 11. We can see that the output polarization angle (open circles) is change abruptly from approximately -25° to 10° when the polarizer is rotated between -20° and 0°. For the same polarizer angles the output ellipticity at low power is changed only by 3° (closed circles). We can conclude that change of the ellipticity of the pump pulse by 3° causes the change of the soliton polarization by 35°, that is compatible with the switch observed in the experiments with the 500 m fiber.

4. Conclusions

The results of the measurements of the polarization of solitons generated in a twisted fiber by the break-up process show that the

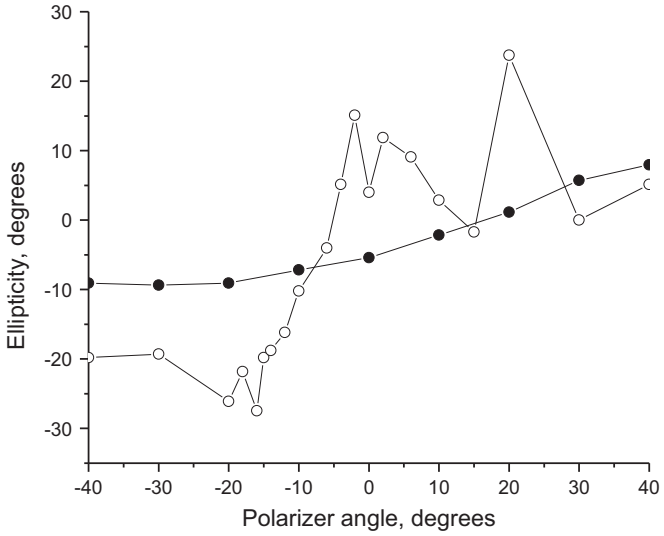

Fig. 11. The dependence of the output ellipticity on the input polarization angle; open circles – ellipticity of solitons; closed circles – output ellipticity of the pump at low power.

dependence of the polarization of solitons on the pump polarization is relatively flat at input ellipticity higher than approximately 15°–20° and fluctuation of the polarization is relatively small. When input ellipticity approach to linear the fluctuation of the polarization grows. We observed an abrupt change of the sign of the ellipticity angle of soliton at input polarization close to linear. The abrupt dependence of the ellipticity of solitons on the input ellipticity assumes that at the input polarization close to linear the solitons tend to have a larger ellipticity angle than the pump pulse.

Acknowledgments

This work is supported by the CONACYT project 130966

References

[1] Y. Silberberg, Y. Barad, Rotating vector solitary waves in isotropic fibers, Opt. Lett. 20 (1995) 246–248.
[2] Curtis R. Menyuk, Stability of solitons in birefringent optical fibers. I. Equal propagation amplitudes, Opt. Lett. 12 (1987) 614–616.
[3] C.R. Menyuk, Stability of soliton in birefringent optical fibers. II. Arbitrary amplitudes, J. Opt. Soc. Am. B 5 (2) (1988) 392–402.
[4] D.N. Christodoulides, R.I. Joseph, Vector solitons in birefringent nonlinear dispersive media, Opt. Lett. 13 (1988) 53–55.
[5] N.N. Akhmediev, A.V. Buryak, J.M. Soto-Crespo, D.R. Andersen, Phase-locked stationary soliton states in birefringent nonlinear optical fibers, JOSA B 12 (1995) 434–439.
[6] J.M. Soto-Crespo, N.N. Akhmediev, B.C. Collings, S.T. Cundiff, K. Bergman, W. H. Knox, Polarization-locked temporal vector solitons in a fiber laser: theory, JOSA B 17 (2000) 366–372.
[7] B.C. Collings, S.T. Cundiff, N.N. Akhmediev, J.M. Soto-Crespo, K. Bergman, W. H. Knox, Polarization-locked temporal vector solitons in a fiber laser: experiment, JOSA B 17 (2000) 354–365.
[8] C. Mou, S. Sergeyev, A. Rozhin, S. Turistyn, All-fiber polarization locked vector soliton laser using carbon nanotubes, Opt. Lett. 36 (2011) 3831–3833.
[9] J.M. Dudley, G. Genty, S. Coen, Supercontinuum generation in photonic crystal fiber, Rev. Mod. Phys. 78 (2006) 1135–1184.
[10] M. Horowitz, Y. Barad, Y. Silberberg, Noiselike pulses with a broadband spectrum generated from an erbium-doped fiber laser, Opt. Lett. 22 (1997) 799–801.
[11] Y. Jeong, L.A. Vazquez-Zuniga, S. Lee, Y. Kwon, On the formation of noise-like pulses in fiber ring cavity configurations, Opt. Fiber Technol. 20 (2014) 575–592.
[12] Rubén Olivier Pottiez, Baldemar Grajales-Coutiño, Evgeny A. Ibarra-Escamilla, Kuzin, Juan Carlos Hernández-García, Adjustable noiselike pulses from a figure-eight fiber laser, Appl. Opt. 50 (2011) E24–E31.
[13] Z. Zhu, T.G. Brown, Polarization properties of supercontinuum spectra generated in birefringent photonic crystal fibers, J Opt. Soc. Am. B 21 (2004) 249–257.
[14] Z. Zhu, T.G. Brown, Experimental studies of polarization properties of supercontinua generated in a birefringent photonic crystal fiber, Opt. Express 12 (2004) 791–796.
[15] M. Lehtonen, G. Genty, H. Ludvigsen, M. Kaivola, Supercontinuum generation in a highly birefringent microstructured fibre, Appl. Phys. Lett. 82 (2003) 2197–2199.
[16] C. Xiong, W.J. Wadsworth, Polarized supercontinuum in birefringent photonic crystal fiber pumped at 1064 nm and application to tunable visible/UV generation, Opt. Express 16 (2008) 2438–2445.
[17] H. Tu, Y. Liu, X. Liu, D. Turchinovich, J. Lægsgaard, S.A. Boppart, Nonlinear polarization dynamics in a weakly birefringent all-normal dispersion photonic crystal fiber: toward a practical coherent fiber supercontinuum laser, Opt. Express 20 (2012) 1113–1128.
[18] D.Y. Tang, L.M. Zhao, B. Zhao, Soliton collapse and bunched noise-like pulse generation in a passively mode-locked fiber ring laser, Opt. Express 13 (2005) 2289–2294.
[19] S. Kobtsev, S. Kukarin, S. Smirnov, S. Turitsyn, A. Latkin, Generation of double-scale femto/pico-second optical lumps in mode-locked fiber lasers, Opt. Express 17 (2009) 20707–20713.
[20] R. Ulrich, A. Simon, Polarization optics of twisted single-mode fibers, Appl. Opt. 18 (1979) 2241–2251.
[21] Diana Tentori, A. Garcia-Weidner, Jones birefringence in twisted single-mode optical fibers, Opt. Express 21 (2013) 31725–31739.
[22] T. Tanemura, K. Kikuchi, Circular-birefringence fiber for nonlinear optical signal processing, J. Lightwave Technol. 24 (2006) 4108–4119.
[23] N. Korneev, E.A. Kuzin, B.A. Villagomez-Bernabe, O. Pottiez, B. Ibarra-Escamilla, A. González-García, M. Durán-Sánchez, Raman-induced polarization stabilization of vector solitons in circularly birefringent fibers, Opt. Express 20 (2012) 24288–24294.
[24] A. Flores-Rosas, J.I. Peralta-Hernandez, Y.E. Bracamontes-Rodríguez, B. A. Villagomez-Bernabe, G. Beltrán-Pérez, O. Pottiez, B. Ibarra-Escamilla, R. Rojas-Laguna, E.A. Kuzin, Observation of a high grade of polarization of solitons generated in the process of pulse breakup in a twisted fiber, JOSA B 31 (2014) 821–826.
[25] E.A. Kuzin, J.M. Estudillo Ayala, B. Ibarra Escamilla, J.W. Haus, Measurements of beat length in short low-birefringence fibers, Opt. Lett. 26 (2001) 1134–1136.
[26] A.J. Barlow, D.N. Payne, The stress-optic effect in optical fibers, IEEE J. Quant. Electron. QE-19 (1983) 834–839.
[27] R. Ulrich, S.C. Rashleigh, W. Eickhoff, Bending-induced birefringence in single-mode fibers, Opt. Lett. 5 (1980) 273–275.